Inorganic Chemistry

Article

pubs.acs.org/IC

Structural Variations in the Uranyl/4,4′-Biphenyldicarboxylate System. Rare Examples of 2D → 3D Polycatenated Uranyl−Organic Networks

Pierre Thuéry*,† and Jack Harrowfield‡

†CEA, IRAMIS, CNRS UMR 3685 NIMBE, LCMCE, Bât. 125, 91191 Gif-sur-Yvette, France

‡ISIS, Université de Strasbourg, 8 allée Gaspard Monge, 67083 Strasbourg, France

Supporting Information

ABSTRACT: 4,4′-Biphenyldicarboxylic acid (H_2L) was reacted with uranyl ions under solvo-hydrothermal conditions with variations in the experimental procedure (organic cosolvent, presence of additional 3d-block metal cations, and N-donor species), thus giving six complexes of the fully deprotonated acid that were characterized by their crystal structure and, in most cases, their emission spectrum. The three complexes $[UO_2(L)(DMA)]$ (**1**), $[UO_2(L)(NMP)]$ (**2**), and $[UO_2(L)(NMP)]$ (**3**) include the cosolvent as a coligand, and they crystallize as two-dimensional (2D) assemblies, with different combinations of the chelating and bridging-bidentate carboxylate coordination modes, resulting in two different topologies. Complex **4**, $[Ni(bipy)_3][(UO_2)_2(L)_2(C_2O_4)]\cdot H_2O$, includes oxalate coligands generated in situ and contains an anionic planar two-dimensional (2D) assembly with a $\{6^3\}$ honeycomb topology. The same hexagonal geometry is found in the homoleptic complexes $[Ni(bipy)_3][(UO_2)_2(L)_3]\cdot 6H_2O$ (**5**) and $[Ni(phen)_3][(UO_2)_2(L)_3]\cdot 4H_2O$ (**6**), but the large size of the hexagonal rings in these cases (~27 Å in the longest dimension) allows 2D → three-dimensional (3D) inclined polycatenation to occur, with the two families of networks either orthogonal in tetragonal complex **5** or at an angle of 73.4° in orthorhombic complex **6**. The parallel networks are arranged in closely spaced groups of two, with possible $\pi\cdots\pi$ stacking interactions, and as many as four rods from four parallel nets pass through each ring of the inclined family of nets, an unusually high degree of catenation. These are the second cases only of 2D → 3D inclined polycatenation in uranyl−organic species. Emission spectra measured in the solid state show the usual vibronic fine structure, with variations in intensity and positions of maxima that are not simply connected with the number of equatorial donors and the presence of additional metal cations.

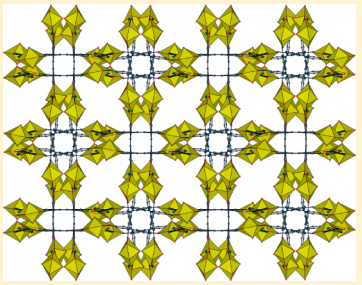

INTRODUCTION

Although uranyl structural chemistry might be thought to be limited by the geometric constraints exerted by the two oxo groups, the high affinity of this cation for a very large array of carboxylate ligands, as well as the diversity of secondary building units resulting from hydrolysis, has allowed remarkable developments in uranyl−organic coordination polymer or framework studies.[1] In this context, we recently explored variations in the experimental procedure as a means of generating different species from a single polycarboxylate ligand. Among these variations, the use of additional alkali, alkaline-earth, d-, p-, or f-block metal cations, often resulting in a dimensionality increase, is well-documented,[1,2] but we also examined the effect of the organic solvent in solvo-hydrothermal methods; this proved to be an interesting approach in several respects. First, the solubility of the ligand may be enhanced in the presence of an organic cosolvent.[3] Second, potentially coordinating solvents may be incorporated into the uranium atom coordination sphere, which is not necessarily adverse to an increase in dimensionality, as shown in several cases for the *N*-methyl-2-pyrrolidone (NMP) cosolvent.[4] Third, solvents such as *N*,*N*-dimethylformamide (DMF) and *N*,*N*-dimethylacetamide (DMA) may be hydrolyzed to give formic acid or acetic acid, respectively, and dimethylamine, these species often finding their way into the compounds formed.[2r,5] Lastly, it has been found that such solvo-hydrothermal conditions are a means of avoiding in a fair measure the hydrolytic formation of oxo- or hydroxo-bridged uranyl oligomers that are very common in uranyl chemistry.[2n,4] Through variation of these additional species (which also commonly include N-donor ligands such as 2,2′-bipyridine[6]) and cosolvents, it was possible to obtain complexes of quite original geometry, such as polynuclear molecular cages and nanotubular polymers with poly(carboxylic acid)s based on the cyclohexyl platform.[7] More recently, we applied the same approach to a ligand containing the biphenyl skeleton, 1,1′-biphenyl-2,2′,6,6′-tetracarboxylic acid, for which planar architectures were mostly obtained, a three-dimensional (3D) framework being formed only with additional lanthanide cations.[8] The work presented here results from attempts to build novel species with another ligand based on the same bis-aromatic motif, 4,4′-biphenyldicarboxylic acid (H_2L), for which two-dimensional (2D) uranyl-containing networks have pre-

Received: June 12, 2015
Published: August 4, 2015

DOI: 10.1021/acs.inorgchem.5b01323
Inorg. Chem. 2015, 54, 8093−8102

Table 1. Crystal Data and Structure Refinement Details

	1	2	3	4	5	6
chemical formula	$C_{18}H_{17}NO_7U$	$C_{19}H_{17}NO_7U$	$C_{19}H_{17}NO_7U$	$C_{60}H_{42}N_6NiO_{17}U_2$	$C_{72}H_{60}N_6NiO_{22}U_2$	$C_{78}H_{56}N_6NiO_{20}U_2$
M (g mol^{-1})	597.35	609.36	609.36	1653.76	1896.03	1932.05
cryst syst	monoclinic	monoclinic	triclinic	monoclinic	tetragonal	orthorhombic
space group	$P2_1/n$	$P2_1/n$	$P\bar{1}$	$C2$	$I\bar{4}c2$	$Fddd$
a (Å)	9.6178(6)	9.9581(5)	14.0825(7)	13.2606(11)	26.3865(6)	32.8519(12)
b (Å)	14.0395(5)	11.8537(4)	16.3562(11)	29.6449(19)	26.3865(6)	44.1088(12)
c (Å)	14.4328(8)	16.0919(9)	18.4268(12)	8.4799(6)	47.5157(17)	46.1720(13)
α (deg)	90	90	84.655(3)	90	90	90
β (deg)	103.813(4)	100.471(3)	78.198(4)	121.965(5)	90	90
γ (deg)	90	90	68.953(3)	90	90	90
V (Å^3)	1892.49(17)	1867.86(15)	3876.6(4)	2828.1(4)	33082.7(19)	66906(4)
Z	4	4	8	2	16	32
D_{calcd} (g cm^{-3})	2.097	2.167	2.088	1.942	1.523	1.534
μ(Mo Kα) (mm^{-1})	8.616	8.732	8.415	6.121	4.201	4.155
F(000)	1120	1144	2288	1584	14752	30016
no. of reflections collected	55534	51551	169991	46648	246327	332102
no. of independent reflections	4858	5688	20005	7130	15684	15864
no. of observed reflections [$I > 2\sigma(I)$]	3129	4188	11814	5617	11926	10303
R_{int}	0.073	0.044	0.100	0.047	0.044	0.046
no. of parameters refined	247	254	1013	395	938	1073
R_1	0.037	0.037	0.038	0.048	0.048	0.053
wR_2	0.070	0.098	0.066	0.126	0.123	0.159
S	0.925	1.058	0.850	1.047	1.037	1.017
$\Delta\rho_{min}$ (e Å^{-3})	−1.19	−1.91	−1.65	−2.09	−0.74	−0.67
$\Delta\rho_{max}$ (e Å^{-3})	0.89	2.71	1.57	1.06	0.92	1.45

viously been described[9] (and a 2D species was also obtained with the related 2,2′-dinitro-4,4′-biphenyldicarboxylic acid,[10] while 3,3′,4,4′-biphenyltetracarboxylic acid gives a one-dimensional complex in which only half the functional groups are coordinated[11]). By using the cosolvent DMF, DMA, or NMP, additional Ni^{2+} or Cu^{2+} cations, and 2,2′-bipyridine (bipy) or 1,10-phenanthroline (phen) donors, we were able to obtain six new uranyl ion complexes with the L^{2-} dicarboxylate, which were characterized by their crystal structure and, in most cases, their emission spectrum at ambient temperature. Surprisingly, two of these complexes display 2D → 3D inclined polycatenation, a phenomenon common enough in metal−organic species,[12] but rare in uranyl chemistry. To the best of our knowledge, only five cases of interpenetration or entanglement in uranyl complexes have been reported,[13] two of which involve 1,4-benzenedicarboxylate (terephthalate),[13a,d] a ligand geometrically close to that used herein, but giving nevertheless different arrangements.

EXPERIMENTAL SECTION

Syntheses. Caution! *Uranium is a radioactive and chemically toxic element, and uranium-containing samples must be handled with suitable care and protection.*

$UO_2(NO_3)_2{\cdot}6H_2O$ (depleted uranium, R. P. Normapur, 99%) and $Ni(NO_3)_2{\cdot}6H_2O$ were purchased from Prolabo, 4,4′-biphenyldicarboxylic acid (H_2L), 1,10-phenanthroline (phen), and $Cu(NO_3)_2{\cdot}2.5H_2O$ were provided by Aldrich, and 2,2′-bipyridine (bipy) was provided by Fluka. Elemental analyses were performed by MEDAC Ltd. at Chobham, U.K.

*[UO_2(L)(DMA)] (**1**).* H_2L (24 mg, 0.10 mmol), $UO_2(NO_3)_2{\cdot}6H_2O$ (50 mg, 0.10 mmol), $Cu(NO_3)_2{\cdot}2.5H_2O$ (24 mg, 0.10 mmol), bipy (16 mg, 0.10 mmol), DMA (0.3 mL), and demineralized water (1.2 mL) were placed in a 10 mL tightly closed glass vessel and heated at 140 °C under autogenous pressure, giving light yellow crystals of complex **1** within 4 days (32 mg, 54% yield). Anal. Calcd for $C_{18}H_{17}NO_7U$: C, 36.19; H, 2.87; N, 2.34. Found: C, 36.29; H, 2.82; N, 2.42.

*[UO_2(L)(NMP)] (**2**).* H_2L (24 mg, 0.10 mmol), $UO_2(NO_3)_2{\cdot}6H_2O$ (50 mg, 0.10 mmol), NMP (0.3 mL), and demineralized water (0.8 mL) were placed in a 10 mL tightly closed glass vessel and heated at 140 °C under autogenous pressure, giving light yellow crystals of complex **2** within 3 weeks, mixed with a small quantity of unreacted H_2L (29 mg, 48% yield). Anal. Calcd for $C_{19}H_{17}NO_7U$: C, 37.45; H, 2.81; N, 2.30. Found: C, 39.20; H, 2.82; N, 2.25. The values found are compatible with the presence of ∼0.15H_2L, in agreement with the presence of a very small amount of white powder adhering to the crystals and resistant to washing (calcd for $C_{21.1}H_{18.5}NO_{7.6}U$: C, 39.25; H, 2.89; N, 2.17).

*[UO_2(L)(NMP)] (**3**).* H_2L (24 mg, 0.10 mmol), $UO_2(NO_3)_2{\cdot}6H_2O$ (50 mg, 0.10 mmol), $Ni(NO_3)_2{\cdot}6H_2O$ (29 mg, 0.10 mmol), bipy (32 mg, 0.20 mmol), NMP (0.3 mL), and demineralized water (0.8 mL) were placed in a 10 mL tightly closed glass vessel and heated at 140 °C under autogenous pressure, giving a low yield of light yellow crystals of complex **3** within 1 week.

*[Ni(bipy)$_3$][(UO_2)$_2$(L)$_2$(C_2O_4)]·H_2O (**4**).* H_2L (24 mg, 0.10 mmol), $UO_2(NO_3)_2{\cdot}6H_2O$ (50 mg, 0.10 mmol), $Ni(NO_3)_2{\cdot}6H_2O$ (29 mg, 0.10 mmol), bipy (32 mg, 0.20 mmol), NMP (0.3 mL), and demineralized water (0.8 mL) were placed in a 10 mL tightly closed glass vessel and heated at 140 °C under autogenous pressure, giving a low yield of light yellow crystals of complex **4** within 2 weeks, mixed with unreacted H_2L.

*[Ni(bipy)$_3$][(UO_2)$_2$(L)$_3$]·$6H_2O$ (**5**).* H_2L (19 mg, 0.08 mmol), $UO_2(NO_3)_2{\cdot}6H_2O$ (25 mg, 0.05 mmol), $Ni(NO_3)_2{\cdot}6H_2O$ (8 mg, 0.03 mmol), bipy (14 mg, 0.09 mmol), DMA (0.3 mL), and demineralized water (1.2 mL) were placed in a 10 mL tightly closed glass vessel and heated at 140 °C under autogenous pressure, giving light yellow crystals of complex **5** within 3 days (31 mg, 61% yield). Anal. Calcd for $C_{72}H_{60}N_6NiO_{22}U_2$: C, 45.61; H, 3.19; N, 4.43. Found: C, 44.95; H, 3.07; N, 3.64. The same complex was obtained when DMA was replaced with DMF.

*[Ni(phen)$_3$][(UO_2)$_2$(L)$_3$]·$4H_2O$ (**6**).* H_2L (24 mg, 0.10 mmol), $UO_2(NO_3)_2{\cdot}6H_2O$ (50 mg, 0.10 mmol), $Ni(NO_3)_2{\cdot}6H_2O$ (29 mg, 0.10 mmol), phen (36 mg, 0.20 mmol), DMF (0.2 mL), and

DOI: 10.1021/acs.inorgchem.5b01323
Inorg. Chem. 2015, 54, 8093−8102

demineralized water (1.0 mL) were placed in a 10 mL tightly closed glass vessel and heated at 140 °C under autogenous pressure, giving a low yield of light orange crystals of complex **6** within 2 weeks.

Crystallography. The data were collected at 150(2) K on a Nonius Kappa-CCD area detector diffractometer[14] using graphite-monochromated Mo Kα radiation (λ = 0.71073 Å). The crystals were introduced into glass capillaries with a protective coating of Paratone-N oil (Hampton Research). The unit cell parameters were determined from 10 frames and then refined on all data. The data (combinations of φ- and ω-scans with a minimum redundancy of 4 for 90% of the reflections) were processed with HKL2000.[15] Absorption effects were corrected empirically with SCALEPACK.[15] The structures were determined either by Patterson map interpretation with SHELXS[16] (**1** and **4**) or by intrinsic phasing with SHELXT[17] (**2**, **3**, **5**, and **6**), expanded by subsequent difference Fourier synthesis and refined by full-matrix least squares on F^2 with SHELXL-2014.[18] All non-hydrogen atoms were refined with anisotropic displacement parameters. The hydrogen atoms bound to oxygen atoms were found on difference Fourier maps, except when indicated below, and the carbon-bound hydrogen atoms were introduced at calculated positions; all hydrogen atoms were treated as riding atoms with an isotropic displacement parameter equal to 1.2 times that of the parent atom (1.5 for CH_3, with optimized geometry). In complex **4**, the water solvent molecule was given an occupancy factor of 0.5 to account for its closeness to its image by symmetry, and its hydrogen atoms were not found. In complex **5**, two solvent water molecules were given occupancy factors of 0.5 to retain acceptable displacement parameters; the water hydrogen atoms were found, except for those of two water molecules. All water molecules in **6** were given partial occupancies (0.5 or 0.25) to retain acceptable displacement parameters and to account for overly close contacts between them. One aromatic ring in **6** is disordered over two positions sharing two opposite carbon atoms, which have been refined with occupancy parameters constrained to sum to unity. Large voids in the lattices of **5** and **6** indicate the presence of other, unresolved water solvent molecules, but because the residual electron density was weak, the SQUEEZE[19] software did not improve the results. The structure of **5** was refined as a two-component inversion twin, with a Flack parameter of 0.518(10). Crystal data and structure refinement parameters are listed in Table 1. The molecular plots were drawn with ORTEP-3[20] and the polyhedral representations with VESTA.[21] The topological analyses were conducted with TOPOS.[22]

Luminescence Measurements. Emission spectra were recorded on solid samples using a Horiba-Jobin-Yvon Fluorolog spectrofluorometer. The powdered complex was pressed between two silica plates that were mounted such that the faces were oriented vertically and at 45° to the incident excitation radiation. An excitation wavelength of 420 nm was used in all cases and the emission monitored between 450 and 650 nm.

RESULTS AND DISCUSSION

Synthesis. The complexes with L^{2-} previously reported, $[UO_2(L)]$, $(NH_4)[(UO_2)_2(L)_2(OH)]\cdot H_2O$, and $[(UO_2)_2(L)(OH)_2]$, were synthesized under hydrothermal conditions at 180 or 200 °C, with addition of aqueous ammonia.[9] In contrast, complexes **1**−**6** were synthesized under solvo-hydrothermal conditions at 140 °C (a value in the middle of the range of temperatures commonly employed). All crystals appeared during the heating phase, and their presence in the glass vials was checked visually. No base was added (except bipy or phen in the cases of compounds **1** and **3**−**6**, these molecules being present in the final species as ligands for Ni^{2+} cations in **4**−**6**), but the H_2L molecule is nevertheless doubly deprotonated in all cases. Use of the relatively extreme conditions of solvo-hydrothermal reactions generally provides a rather useful means of overcoming solubility problems frequently associated with reactions between materials of very different chemical characteristics. In the case of uranyl ion complexes of weakly basic ligands such as carboxylates, it is useful for avoiding the formation of gels often obtained from the reaction of uranyl species with alkali metal carboxylates, effectively exploiting the enhanced ionization of the acid at high temperatures to obtain the carboxylate anion in the absence of hydroxide. There are disadvantages associated with these procedures in that materials soluble only under high pressure and temperature may precipitate if the reaction mixture is returned to normal conditions and in that very limited thermodynamic data are available for the conditions used, so that it is usually necessary to proceed in a rather empirical manner to optimize any synthesis.

Among the many combinations of organic solvents (DMF, DMA, NMP, CH_3CN, and CH_3OH), additional cations (Mn^{2+}, Co^{2+}, Ni^{2+}, Cu^{2+}, and Tb^{3+}), and nitrogen donors (bipy and phen) that have been tested, only the six reported gave crystalline material of suitable quality for structural determination, the most frequent outcome of the reaction being the formation of amorphous precipitates. In addition, the yields are very low for compounds **3**, **4**, and **6**, and the presence of small amounts of impurities is shown by elemental analyses of **2** and **5**. These six complexes were obtained with either DMF (**6**), DMA (**1** and **5**), or NMP (**2**−**4**) as the cosolvent, these molecules being bound to uranyl ions in **1**−**3**. In all cases but **2**, a 3d-block metal cation was present during the synthesis, and it is retained as the $Ni(bipy/phen)_3^{2+}$ counterion in **4**−**6**. It is notable that L^{2-} is always bound to uranyl ions only, and that no heterometallic complex is formed; the usefulness of additional cations as a means of increasing the dimensionality of the species formed is thus not apparent here. The solution chemistry involved in solvo-hydrothermal syntheses is undoubtedly rather complicated, and it is not clear exactly what factors may have influenced the solubility of the crystalline materials isolated in this work. Complexes **1** and **3**, for example, crystallized in the presence of Cu(II) and Ni(II) and different quantities of 2,2′-bipyridine but without incorporation of these reagents, so that the influence of the latter must presumably be due to effects, such as changes in solution acidity or in the availability of uncoordinated L^{2-}, which might determine both the rate and extent of product crystallization. None of the complexes contains oxo or hydroxo anions, but oxalate anions were formed in situ during the synthesis of **4**, which is a common occurrence in hydrothermal syntheses.[2k,23] The pathway to oxalate formation is somewhat obscure, especially when a mixture of organic substrates for oxidation is present, and has been elucidated only in some particular cases.[23n,o] The complexity of factors influencing solvothermal synthesis is nicely illustrated here by the fact that increasing the Ni(II):bipy ratio from 1:2 in the case of the synthesis of complex **4** to 1:3 in the case of **5** leads to a considerably increased yield of a solid containing the $[Ni(bipy)_3]^{2+}$ cation but also to a change in the composition of the associated anion.

Crystal Structures. The three complexes $[UO_2(L)(DMA)]$ (**1**) and $[UO_2(L)(NMP)]$ (**2** and **3**) are structurally close to one another, although they were obtained either from uranyl ions alone (**2**) or with additional Cu^{2+} or Ni^{2+} cations and bipy molecules present (**1** and **3**), and they are shown in Figures 1−3. The asymmetric unit contains one formula unit in **1** and **2**, and four in **3**, the four independent uranium atoms in the last case being in similar environments. The uranyl ions in **1**−**3** are chelated by one carboxylate group and bound to two oxygen atoms from two more L^{2-} ligands and the oxygen donor of the solvent molecule, which gives the usual pentagonal bipyramidal

DOI: 10.1021/acs.inorgchem.5b01323
Inorg. Chem. 2015, 54, 8093−8102

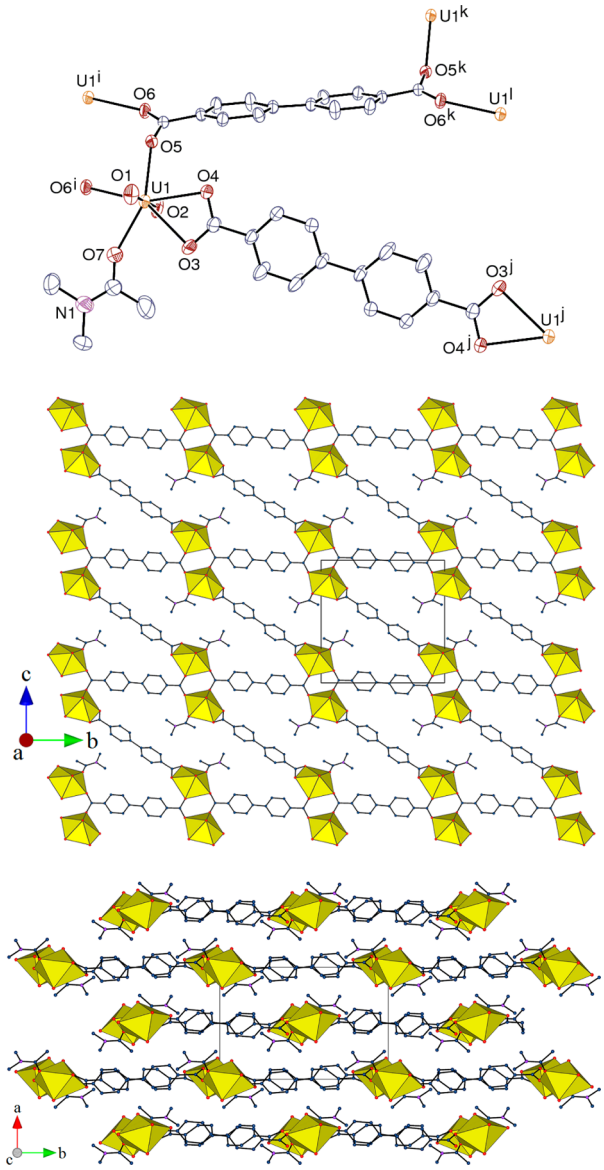

Figure 1. View of complex **1** (top). Displacement ellipsoids are drawn at the 40% probability level. Symmetry codes: $i = 1 - x, 1 - y, 1 - z$; $j = 1 - x, -y, -z$; $k = 1 - x, -y, 1 - z$; $l = x, y - 1, z$. View of the 2D assembly (middle). View of the packing with layers viewed edge-on (bottom). The uranium coordination polyhedra are shown in the last two views. Hydrogen atoms have been omitted from all views.

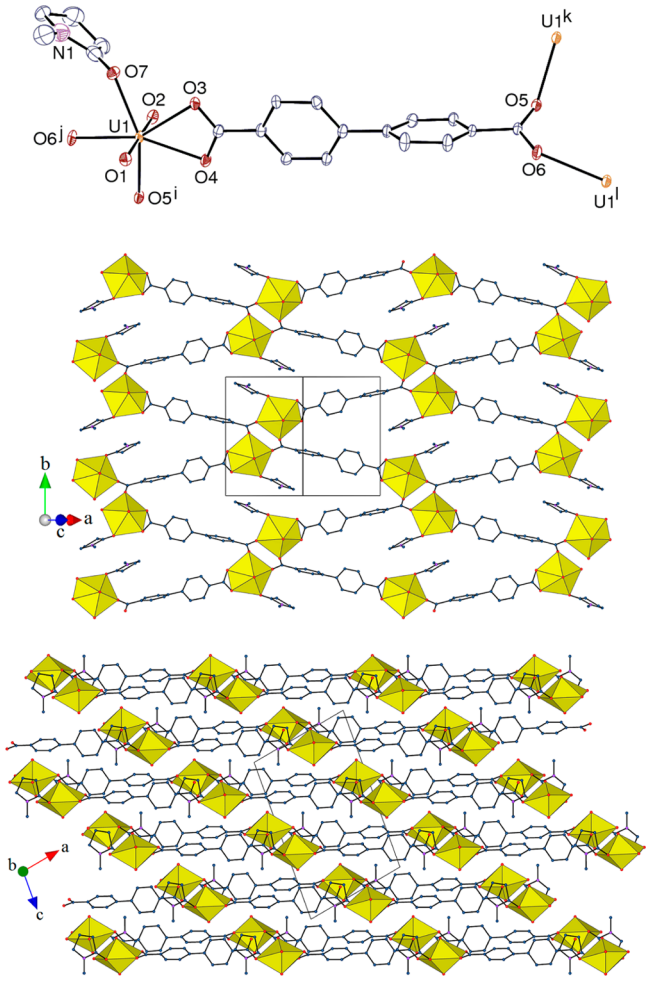

Figure 2. View of complex **2** (top). Displacement ellipsoids are drawn at the 30% probability level. Symmetry codes: $i = {}^{3}/_{2} - x, y - {}^{1}/_{2}, {}^{3}/_{2} - z$; $j = x - {}^{3}/_{2}, {}^{3}/_{2} - y, z - {}^{1}/_{2}$; $k = {}^{3}/_{2} - x, y + {}^{1}/_{2}, {}^{3}/_{2} - z$; $l = x + {}^{3}/_{2}, {}^{3}/_{2} - y, z + {}^{1}/_{2}$. View of the 2D assembly (middle). View of the packing with layers viewed edge on (bottom). Hydrogen atoms have been omitted from all views.

uranium environment. The U−O(carboxylate) bond lengths are in the ranges of 2.406(4)−2.496(4) Å [average of 2.46(2) Å] for chelating groups and 2.308(3)−2.383(3) Å [average of 2.33(2) Å] for bridging-bidentate ones, these values being unexceptional, as are those for the terminal ligands, 2.312(5) Å for DMA and 2.338(3)−2.406(3) Å [average of 2.38(2) Å] for NMP. Three different coordination modes of the L^{2-} ligand are found. The asymmetric unit contains two L^{2-} halves in complex **1**, the complete ligands being centrosymmetric, with the result that one of them is doubly chelating and the other doubly bridging-bidentate. The single ligand in **2** is both chelating and bridging-bidentate, while two of the four independent ligands in **3** are doubly chelating and the other two doubly bridging-bidentate, as in **1**. The dihedral angles between the two aromatic rings span a wide range, from 0° in **1** to 69.25(18)° in **2**, with intermediate values of 19.4(3)−45.8(2)° in **3**, and the COO groups are tilted with respect to the ring to which they are attached, with dihedral angles in the range of 3.9(8)−25.7(3)°. The L^{2-} dianions connect either two, three, or four metal cations, while the connectivity of the latter is unchanged, all being bound to three L^{2-} ligands. In all cases, uranyl dimers with double carboxylate bridges are formed, which are assembled through further bridging into 2D assemblies parallel to (1 0 0), (1 0 $\bar{3}$), and (1 1 2) in **1**−**3**, respectively. The difference in ligand connectivity results in different total point (Schläfli) symbols, $\{4.6^2\}_2\{4^2.6^2.8^2\}$ in **1** and **3** (first symbol for metal cations and second for doubly bridging-bidentate ligands; doubly chelating ligands are considered as edges) and $\{4.8^2\}$ in **2**. As shown in the nodal representations of Figure 4, the network in **1** and **3**, which includes three- and four-fold nodes as well as simple edges, displays rows of uranyl dimers connected to one another by the doubly bridging-bidentate ligands, these rows being assembled into a layer through the bis-chelating ligands. In contrast, the uranyl dimers in **2** are arranged in staggered rows and all nodes are three-fold ones. No significant $\pi\cdots\pi$ stacking interaction is present in any of the three compounds. In **1**, two CH$\cdots\pi$ contacts at ∼2.9 Å may reflect significant interactions between one methyl group of

DOI: 10.1021/acs.inorgchem.5b01323
Inorg. Chem. 2015, 54, 8093−8102

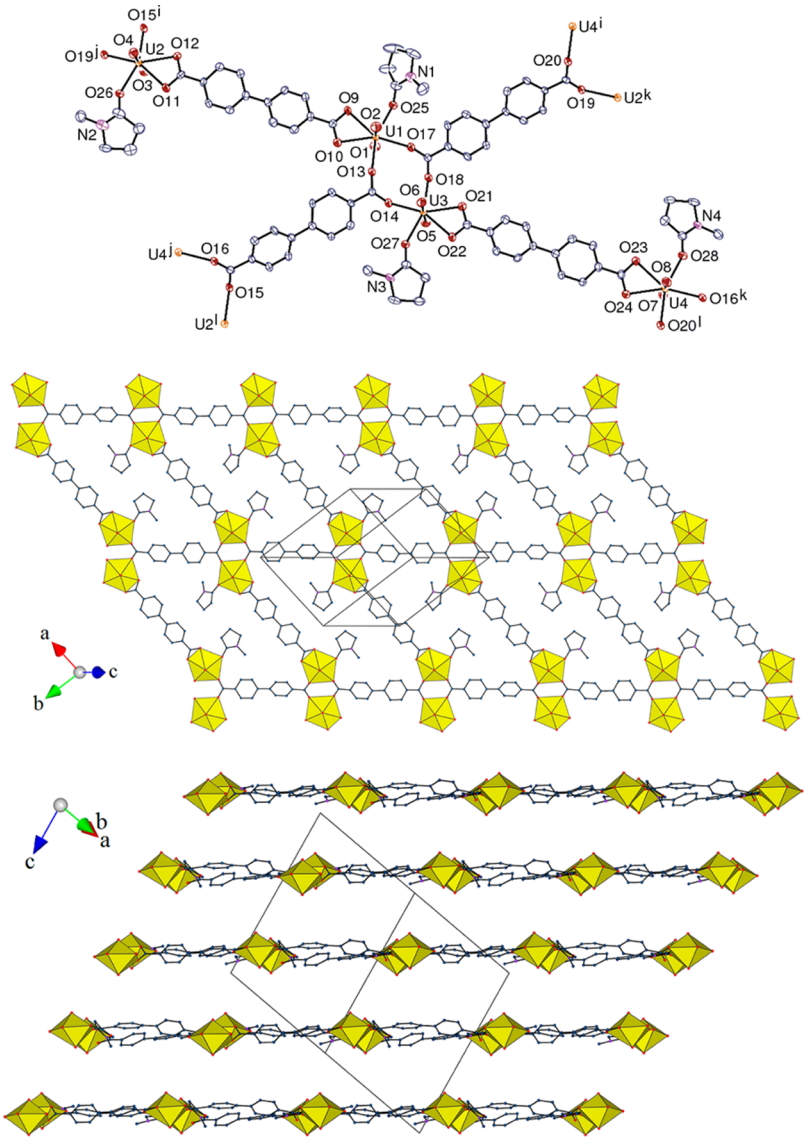

Figure 3. View of complex **3** (top). Displacement ellipsoids are drawn at the 50% probability level. Symmetry codes: $i = x - 1, y + 1, z$; $j = x - 2, y, z + 1$; $k = x + 2, y, z - 1$; $l = x + 1, y - 1, z$. View of the 2D assembly (middle). View of the packing with layers viewed edge on (bottom). Hydrogen atoms have been omitted from all views.

DMA and two aromatic rings pertaining to either the same layer or an adjacent layer. The situation is comparable in **2**, with one possibly significant contact at ∼3.0 Å between one hydrogen atom of the NMP methyl group and an aromatic ring in an adjacent layer, while in **3**, one aromatic and one NMP methyl hydrogen atom are involved in contacts at ∼2.8 and 3.0 Å with aromatic rings in one adjacent layer. The Kitaigorodski packing indices (KPIs, estimated with PLATON[19]) are 0.67, 0.70, and 0.68 in **1**−**3**, respectively, indicating a slightly more compact packing in **2**.

While the uranyl−organic assembly is neutral in **1**−**3**, it is anionic and $Ni(bipy/phen)_3^{2+}$ counterions are present in the three other compounds. The complex $[Ni(bipy)_3][(UO_2)_2(L)_2(C_2O_4)]\cdot H_2O$ (**4**), represented in Figure 5, includes additional oxalate ligands. The asymmetric unit contains two uranium atoms and one nickel atom, all located on a 2-fold rotation axis, one doubly chelating L^{2-} ligand, and half an oxalate ligand. Both uranium atoms are in hexagonal bipyramidal environments, being chelated by two L^{2-} and one oxalate ligands, with U−O(carboxylate) bond lengths in the range of 2.41(2)−2.505(13) Å [average of 2.47(3) Å]. Dimers of oxalate-bridged uranyl ions are formed, each of them being bound to four neighbors by L^{2-} ligands to give a 2D assembly parallel to (2 0 1) and with the point symbol $\{6^3\}$ (if the ligands are considered as edges, or $\{12^3\}_2\{12\}_3$ if they are considered as nodes, with the first symbol for uranium atoms and the second for the ligands). This topology is similar to that found in a uranyl complex with oxalate anions only.[6] The packing defines channels parallel to the [0 0 1] axis (tilted with respect to the 2D networks), which are occupied by the counterions (the nickel centers being located between the layers). The L^{2-} ligand deviates from planarity, with dihedral angles of 22.4(13)° between the aromatic rings, and 25(4) and 21(3)° between the COO groups and the aromatic rings. In contrast to the previous cases, $\pi\cdots\pi$ stacking interactions may be present in **4**, between the aromatic ring bearing the O3/O4 carboxylate group and its image pertaining to an adjacent layer [centroid···centroid distance of 3.577(15) Å]; no CH···π interaction is apparent. The KPI of 0.69 indicates that no free space is present.

DOI: 10.1021/acs.inorgchem.5b01323
Inorg. Chem. 2015, 54, 8093−8102

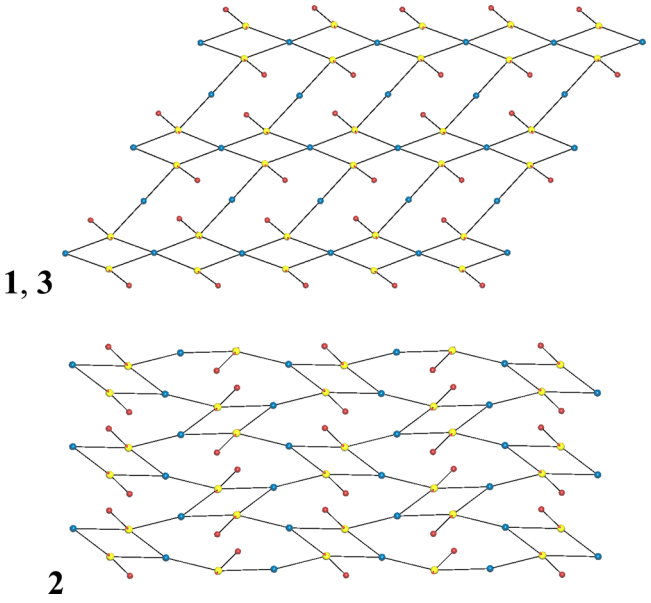

Figure 4. Nodal representation of the 2D networks in complexes **1** and **3** (top) and **2** (bottom): yellow for uranium, red for oxygen, blue for the centroid of the L^{2-} ligand, and dark red for the centroid of the DMA or NMP molecule.

The two complexes $[Ni(bipy)_3][(UO_2)_2(L)_3]\cdot 6H_2O$ (**5**) and $[Ni(phen)_3][(UO_2)_2(L)_3]\cdot 4H_2O$ (**6**) are derived from **4** by replacement of the oxalate bridges with a third L^{2-} ligand (Figures 6–8). In both cases, the two crystallographically independent uranyl ions are chelated by three carboxylate groups, giving a uranium hexagonal bipyramidal geometry, with U–O(carboxylate) bond lengths in the range of 2.406(10)–2.503(8) Å [average of 2.45(2) Å]. The uranyl cations are thus three-fold nodes and the ligands two-fold ones (i.e., edges), and a 2D network is formed, with the same $\{6^3\}$ topology as in complex **4**. The hexagonal honeycomb (hcb) network is topologically analogous to that in complex **4**, but replacement of oxalate with L^{2-} ligand bridges results in an increase in size of the rings: while the largest and smallest dimensions in **4** are ~24 and 18 Å, respectively, those in **5** and **6** are ~27 and 22/23 Å, respectively (Figure 6). It is notable that, although uranyl-containing hexagonal networks are quite common, they are often built from smaller rings that include three cations and three anions, all being three-fold nodes,[7b,c] instead of six of each as in the cases presented here. The large size of the rings in **5** and **6** has the interesting consequence of allowing polycatenation (Hopf links) to occur. Complex **5** crystallizes in tetragonal space group $I\bar{4}c2$, and two sets of orthogonal 2D assemblies, related to one another by the 4-fold rotoinversion axis, run parallel to either (1 0 0) or (0 1 0) (Figure 7). In complex **6**, which crystallizes in orthorhombic space group *Fddd*, the two sets are related to one another by the diamond glide planes and they are parallel to (1 $\bar{1}$ 0) or (1 1 0), thus making a dihedral angle of 73.4° (Figure 8). Both sets of networks interpenetrate in the 2D + 2D → 3D inclined polycatenation mode, with [0 0 1] as zone direction in the two complexes. What is more unusual is that parallel networks are arranged in groups of two spatially close and offset units, related to one another by the 2-fold rotation axis parallel to [0 0 1]. As shown in the nodal representation in Figure 9, four L^{2-} rods pertaining to four rings of one subset (two groups of two closely associated ones) pass through each ring of the other, inclined subset, which

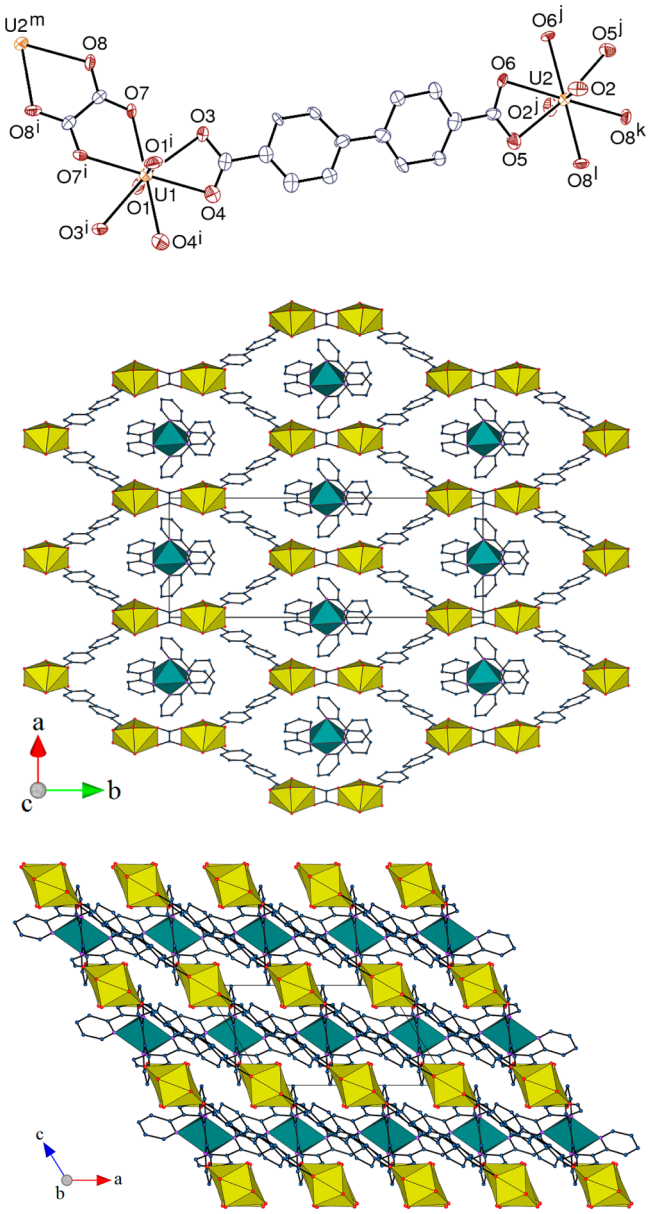

Figure 5. View of complex **4** (top). Displacement ellipsoids are drawn at the 50% probability level. Counterions, solvent molecules, and hydrogen atoms have been omitted. Symmetry codes: $i = -x, y, -z$; $j = 1 - x, y, -z - 2$; $k = x + {}^1/_2, y + {}^1/_2, z - 1$; $l = {}^1/_2 - x, y + {}^1/_2, -z - 1$; $m = x - {}^1/_2, y - {}^1/_2, z + 1$. View of the 2D assembly with the counterions (middle). View of the packing with layers viewed edge on (bottom). Uranium coordination polyhedra are yellow and those of nickel green; solvent molecules and hydrogen atoms have been omitted from the bottom two views.

represents an unusually high degree of catenation.[12g] Conversely, each rod passes through two rings from a close set of planes. The counterions are located in the voids separating the groups of two 2D assemblies (Figures 7 and 8), the slight difference in size resulting from the replacement of bipy in **5** with phen in **6** being probably the origin of the different symmetry of the lattices. The KPI values of ~0.32, with counterions and solvent molecules omitted, show that the entangled species are far from filling the whole volume, and the values of ~0.58, when the cations and solvents are present, are indicative of free spaces being retained, which are probably occupied by disordered water molecules. Here also, the dihedral

DOI: 10.1021/acs.inorgchem.5b01323
Inorg. Chem. 2015, 54, 8093–8102

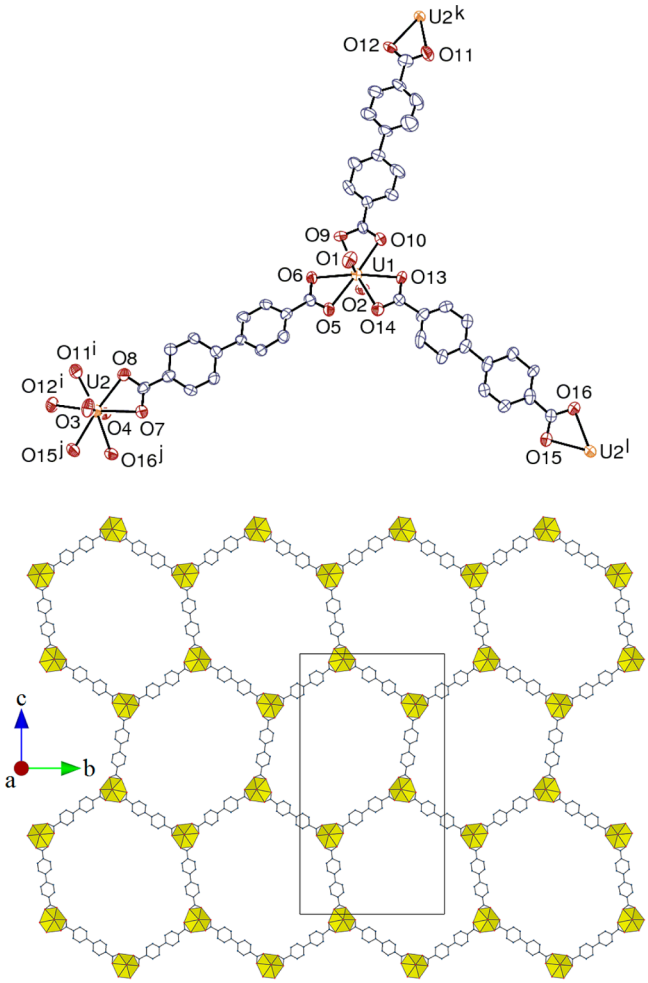

Figure 6. View of complex **5** (top). Displacement ellipsoids are drawn at the 50% probability level. Counterions, solvent molecules, and hydrogen atoms have been omitted. Symmetry codes: $i = x, -y, z + {}^1/_2$; $j = x, 1 - y, z + {}^1/_2$; $k = x, -y, z - {}^1/_2$; $l = x, 1 - y, z - {}^1/_2$. View of the 2D assembly (bottom).

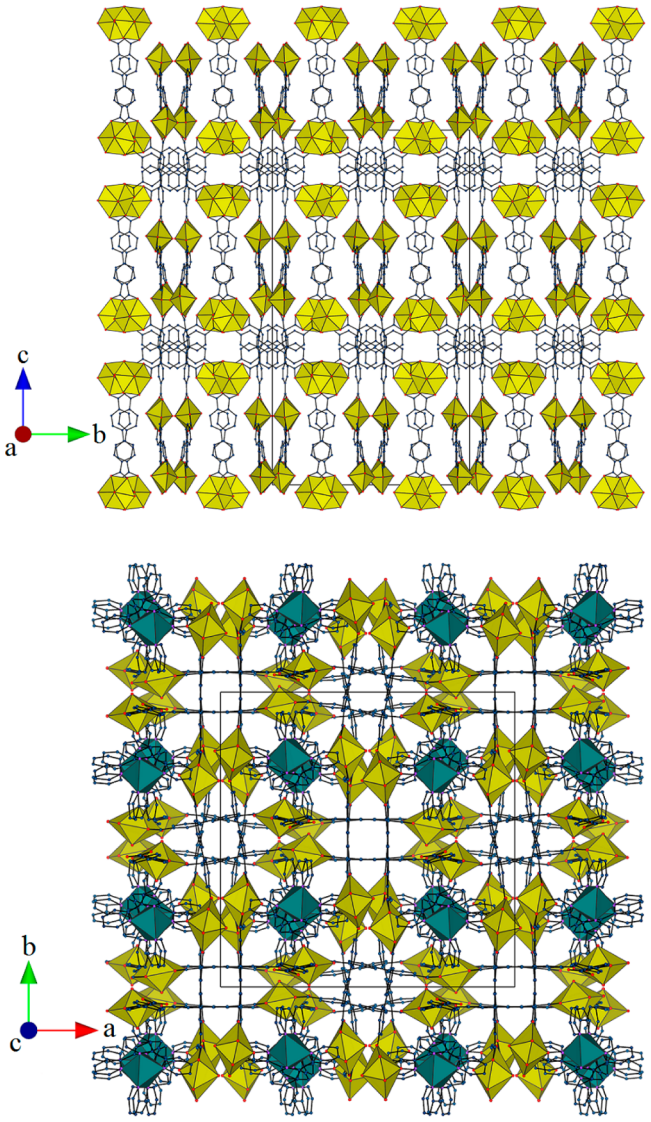

Figure 7. Two orthogonal views of the entanglement in complex **5**, with one family of 2D networks viewed side on and the other edge on, and counterions excluded (top) or with both families edge on and counterions present (bottom). Uranium coordination polyhedra are colored yellow and those of nickel green; solvent molecules and hydrogen atoms have been omitted.

angles between the aromatic rings in the L^{2-} ligands span a wide range, 4.45(9)−31.7(3)° (both extreme values in complex **5**), while the angles between the COO groups and the aromatic rings are in the range of 3.1(4)−19.6(14)° [the largest value being for a disordered molecule; all other values are less than 10.1(2)°]. Possibly significant $\pi\cdots\pi$ stacking and CH$\cdots\pi$ interactions are found in these structures. Some of the former involve one aromatic ring from L^{2-} and one from bipy or phen, but others (two in **5** and three in **6**) are between L^{2-} ligands pertaining to each member of the close parallel nets [centroid$\cdots$centroid distance of 3.702(9)−4.228(5) Å]. All the possible CH$\cdots\pi$ interactions associate one L^{2-} ligand and one bipy or phen molecule (H$\cdots$centroid distance of 2.67−3.00 Å, C−H$\cdots$centroid angle of 140−158°). The solvent water molecules are very disordered in **6**, and partially in **5**, but interestingly, one of them in the latter case makes a direct link between two nets inclined with respect to one another [O17$\cdots$O1 2.903(15) Å, O17−H$\cdots$O1 143°; O17$\cdots$O9^i 3.045(16) Å, O17−H$\cdots$O9^i 148°, where $i = -y, x, 1 - z$].

As indicated in the Introduction, only five cases of interpenetrating uranyl−organic assemblies are known. In the first reported case, 1,4-benzenedicarboxylate was used to generate a 2D assembly with the $\{6^3\}$ topology, similar to that in **5** and **6**, but with smaller rings due to the smaller length of the ligands; the interpenetration is of the 2D → 2D parallel type, with only one rod passing through each ring and no increase in dimensionality.[13a] In the second case, the ligand is isonicotinate *N*-oxide and the 2D assemblies resulting from coordination and hydrogen bonding display a 2D → 2D parallel entanglement.[13b] Three-fold interpenetration of 3D frameworks has been achieved with semirigid tri- and hexacarboxylates,[13c] and in another complex with 1,4-benzenedicarboxylate.[13d] Lastly, 3-fold 2D → 3D inclined polycatenation has been observed with the 3,5-di(4′-carboxyphenyl)benzoate ligand; in this case, the rings are much smaller than in complexes **5** and **6**, with an ∼10 Å width, because they are built from only three cations and three ligands (these being three-fold nodes), and as a consequence, only one cationic node of one network is located within the ring of another network.[13e] In the latter case, the undulating shape of the 2D assemblies was probably important in the formation of the polycatenated

DOI: 10.1021/acs.inorgchem.5b01323
Inorg. Chem. 2015, 54, 8093−8102

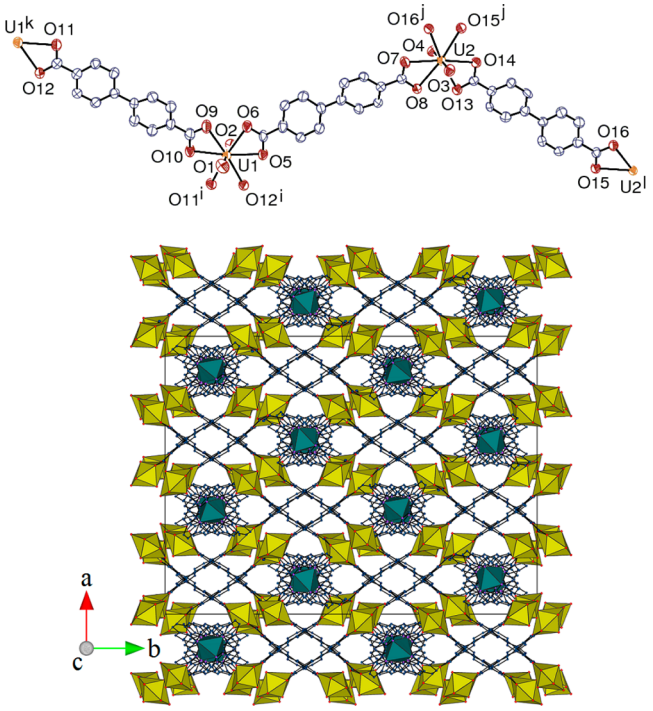

Figure 8. View of complex **6** (top). Displacement ellipsoids are drawn at the 50% probability level. Counterions, solvent molecules, and hydrogen atoms have been omitted. Symmetry codes: $i = x - {}^1/_4, y - {}^1/_4, 1 - z$; $j = x + {}^1/_4, y + {}^1/_4, 2 - z$; $k = x + {}^1/_4, y + {}^1/_4, 1 - z$; $l = x - {}^1/_4, y - {}^1/_4, 2 - z$. View of the entanglement with the two families of 2D networks shown edge on (bottom). Uranium coordination polyhedra are colored yellow and those of nickel green; solvent molecules and hydrogen atoms have been omitted.

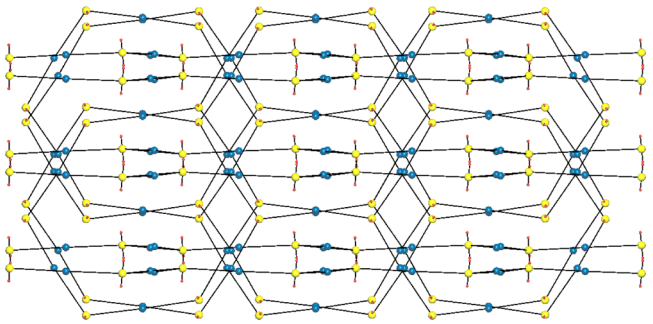

Figure 9. Nodal representation of the polycatenation of networks in complex **5** (similar to that in complex **6**), viewed down the [1 0 0] axis and with the zone direction [0 0 1] horizontal: yellow for uranium, red for oxygen, and blue for the centroid of the L^{2-} ligand.

system, because the planar geometry of those obtained with the related ligand 1,3,5-tris(4′-carboxyphenyl)benzoate leads to association through $\pi\cdots\pi$ stacking interactions. This is not observed here because the 2D assemblies in **4** as well as in **5** and **6** are all close to planarity. The long and rigid (except for rotations of the aromatic rings and functional groups along the main axis) L^{2-} ligand is of course well adapted to the formation of large rings, which themselves are conducive to interpenetration or polycatenation. Rigidity is an essential property in this case, and it may be noted that the long but highly flexible aliphatic dicarboxylic acids have not given any interpenetrated uranyl–organic assembly until now.[24]

Luminescence Properties. Emission spectra under excitation at a wavelength of 420 nm, a value suitable for uranyl excitation,[25] were recorded in the solid state for all compounds except **3** and **6**, for which a sufficient amount of crystals could not be isolated, and they are represented in Figure 10. In all cases, the typical vibronic progression corresponding to the $S_{11} \rightarrow S_{00}$ and $S_{10} \rightarrow S_{0\nu}$ (ν = 0–4) electronic transitions[26] is observed. Although the number of donor atoms in the uranyl equatorial plane is known to affect the position of the maxima,[2r,4,5,27] the spectra of **1**, **2** (five equatorial donors), and **4** (six donors) are essentially identical, with the four main emission bands located at 492 (s), 512 (s), 536 (m), and 561 (w) nm. In contrast, the emission of **5** (six equatorial donors) is much less intense, and the positions of the major peaks, at 464 (m), 480 (s), 499 (s), and 521 (m) nm, are blue-shifted with respect to the former ones and close to those observed for other uranyl carboxylate complexes with six equatorial donors.[7c] The lower resolution in the spectrum of **5** could be attributed to the presence of two crystallographically independent uranyl ions, although their environments are similar, but this is clearly uncertain because no such effect is observed in **4**. Quenching of uranyl emission by transition metal cations has been reported,[2m,n,r,4,8,28] but it is not always observed, as shown here by the intense and well-resolved spectrum of complex **4**; however, it may be effective in significantly reducing the emission intensity in complex **5**.

CONCLUSIONS

Variations in the experimental conditions (organic cosolvent, additional 3d-block metal cations, and nitrogen donors) allowed the synthesis of six novel uranyl ion complexes with 4,4′-biphenyldicarboxylate (L^{2-}) by solvo-hydrothermal methods. In common with the complexes previously described in this system,[9] all the present species crystallize as 2D assemblies, but with different topologies due to the presence of coordinated solvents (DMA in **1** and NMP in **2** and **3**), oxalate coligands formed in situ (**4**), or $Ni(bipy/phen)_3^{2+}$ counterions (**4**–**6**). While L^{2-} had been found to be coordinated in a doubly bridging-bidentate mode in the previous complexes, three coordination modes are found here, doubly chelating (**1** and **3**–**6**), doubly bridging-bidentate (**1** and **3**), and chelating/bridging-bidentate (**2**). Although this ligand is obviously well suited to build 2D coordination polymers with uranyl and is not fit in any straightforward way to give 3D frameworks, an interesting increase in dimensionality is nevertheless obtained through polycatenation, a rare phenomenon in uranyl structural chemistry. Hexagonal honeycomb networks are present in complexes **4**–**6**, with the rings smaller in **4** (due to the presence of oxalate coligands) than in **5** and **6**. The very large size of these rings in the two latter compounds allows 2D → 3D inclined polycatenation to occur, with four rods from four parallel networks passing through each ring of an inclined one. Only one example of inclined polycatenation in an uranyl–organic assembly has recently been reported, and this is quite different because three families of nets are present and the smaller-sized rings are occupied by only one node of one of the inclined nets.[13e] These results further illustrate the interest in varying the experimental procedure to generate novel and sometimes very original species for a given uranyl/ligand system. The emission spectra of complexes **1**, **2**, **4**, and **5** show the usual vibronic progression, with variations in intensity and positions of maxima that are not simply connected with the

DOI: 10.1021/acs.inorgchem.5b01323
Inorg. Chem. 2015, 54, 8093–8102

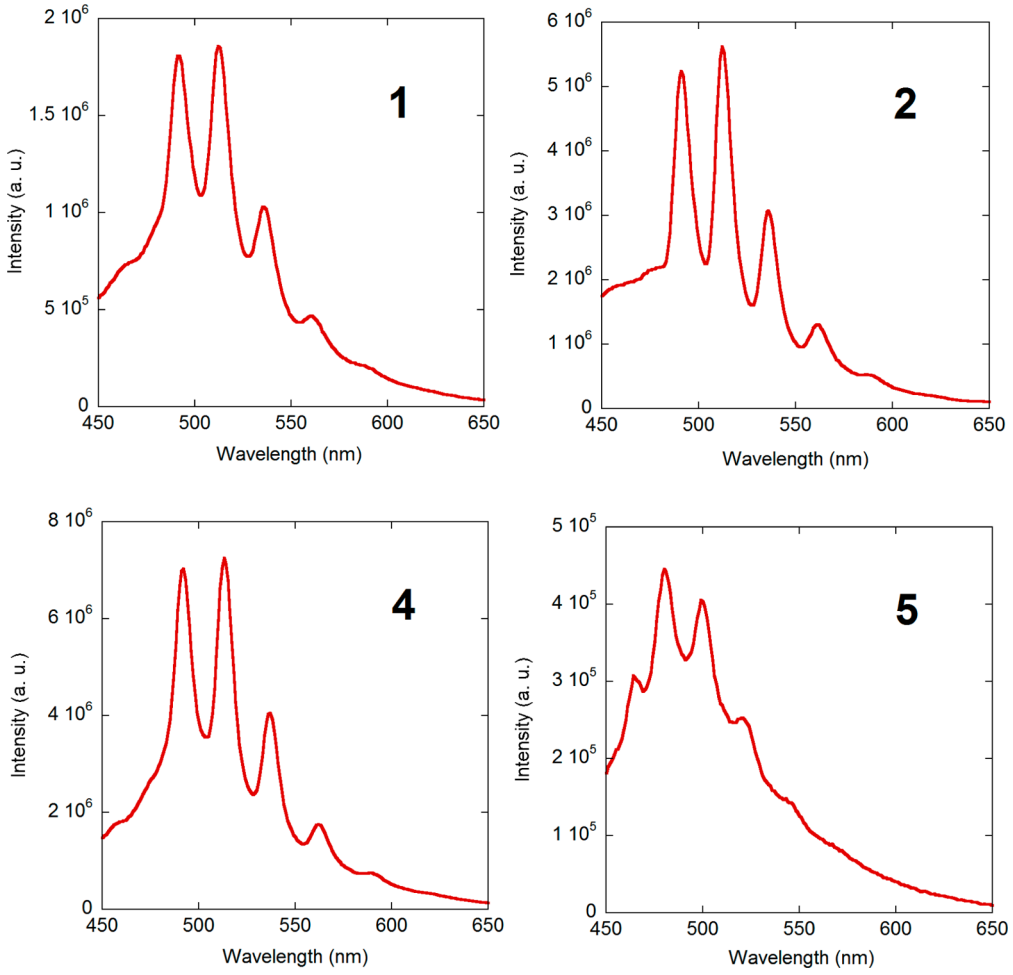

Figure 10. Solid state emission spectra of complexes **1**, **2**, **4**, and **5**. The excitation wavelength was 420 nm.

number of equatorial donors and the presence of additional metal cations.

■ ASSOCIATED CONTENT

Supporting Information

Tables of crystal data, atomic positions, and displacement parameters, anisotropic displacement parameters, and bond lengths and bond angles in CIF format. The Supporting Information is available free of charge on the ACS Publications website at DOI: 10.1021/acs.inorgchem.5b01323.

■ AUTHOR INFORMATION

Corresponding Author

*E-mail: pierre.thuery@cea.fr.

Notes

The authors declare no competing financial interest.

■ REFERENCES

(1) (a) Cahill, C. L.; de Lill, D. T.; Frisch, M. *CrystEngComm* **2007**, *9*, 15−26. (b) Cahill, C. L.; Borkowski, L. A. In *Structural Chemistry of Inorganic Actinide Compounds*; Krivovichev, S. V., Burns, P. C., Tananaev, I. G., Eds.; Elsevier: Amsterdam, 2007; Chapter 11. (c) Wang, K. X.; Chen, J. S. *Acc. Chem. Res.* **2011**, *44*, 531−540. (d) Andrews, M. B.; Cahill, C. L. *Chem. Rev.* **2013**, *113*, 1121−1136. (e) Loiseau, T.; Mihalcea, I.; Henry, N.; Volkringer, C. *Coord. Chem. Rev.* **2014**, *266*−*267*, 69−109. (f) Su, J.; Chen, J. S. *Struct. Bonding (Berlin)* **2015**, *163*, 265−296.

(2) For some recent examples, see: (a) Masci, B.; Thuéry, P. *CrystEngComm* **2008**, *10*, 1082−1087. (b) Masci, B.; Thuéry, P. *Cryst. Growth Des.* **2008**, *8*, 1689−1696. (c) Thuéry, P. *Inorg. Chem. Commun.* **2009**, *12*, 800−803. (d) Thuéry, P. *Cryst. Growth Des.* **2009**, *9*, 4592−4594. (e) Thuéry, P. *Cryst. Growth Des.* **2010**, *10*, 2061−2063. (f) Volkringer, C.; Henry, N.; Grandjean, S.; Loiseau, T. *J. Am. Chem. Soc.* **2012**, *134*, 1275−1283. (g) Mihalcea, I.; Volkringer, C.; Henry, N.; Loiseau, T. *Inorg. Chem.* **2012**, *51*, 9610−9618. (h) Olchowka, J.; Falaise, C.; Volkringer, C.; Henry, N.; Loiseau, T. *Chem. - Eur. J.* **2013**, *19*, 2012−2022. (i) Olchowka, J.; Volkringer, C.; Henry, N.; Loiseau, T. *Eur. J. Inorg. Chem.* **2013**, 2109−2114. (j) Thuéry, P. *CrystEngComm* **2013**, *15*, 6533−6545. (k) Thuéry, P.; Rivière, E. *Dalton Trans.* **2013**, *42*, 10551−10558. (l) Hou, Y. N.; Xu, X. T.; Xing, N.; Bai, F. Y.; Duan, S. B.; Sun, Q.; Wei, S. Y.; Shi, Z.; Zhang, H. Z.; Xing, Y. H. *ChemPlusChem* **2014**, *79*, 1304−1315. (m) Kerr, A. T.; Cahill, C. L. *Cryst. Growth Des.* **2014**, *14*, 1914−1921. (n) Thuéry, P.; Harrowfield, J. *CrystEngComm* **2014**, *16*, 2996−3004. (o) Kerr, A. T.; Cahill, C. L. *Cryst. Growth Des.* **2014**, *14*, 4094−4103. (p) Thuéry, P.; Harrowfield, J. *Eur. J. Inorg. Chem.* **2014**, 4772−4778. (q) Weng, Z.; Zhang, Z. H.; Olds, T.; Sterniczuk, M.; Burns, P. C. *Inorg. Chem.* **2014**, *53*, 7993−7998. (r) Thuéry, P.; Rivière, E.; Harrowfield, J. *Inorg. Chem.* **2015**, *54*, 2838−2850.

(3) Thuéry, P.; Masci, B.; Harrowfield, J. *Cryst. Growth Des.* **2013**, *13*, 3216−3224.

(4) Thuéry, P.; Harrowfield, J. *Cryst. Growth Des.* **2014**, *14*, 1314−1323.

(5) Thuéry, P.; Harrowfield, J. *CrystEngComm* **2015**, *17*, 4006−4018.

(6) Thuéry, P. *Eur. J. Inorg. Chem.* **2013**, 4563−4573.

DOI: 10.1021/acs.inorgchem.5b01323
Inorg. Chem. 2015, 54, 8093−8102

(7) (a) Thuéry, P. *Cryst. Growth Des.* **2014**, *14*, 901−904. (b) Thuéry, P. *Cryst. Growth Des.* **2014**, *14*, 2665−2676. (c) Thuéry, P.; Harrowfield, J. *Cryst. Growth Des.* **2014**, *14*, 4214−4225.
(8) Thuéry, P.; Harrowfield, J. *Inorg. Chem.* **2015**, *54*, 6296−6305.
(9) (a) Mihalcea, I.; Henry, N.; Bousquet, T.; Volkringer, C.; Loiseau, T. *Cryst. Growth Des.* **2012**, *12*, 4641−4648. (b) Cantos, P. M.; Jouffret, L. J.; Wilson, R. E.; Burns, P. C.; Cahill, C. L. *Inorg. Chem.* **2013**, *52*, 9487−9495.
(10) Qu, Z. R. *Chin. J. Inorg. Chem.* **2007**, *10*, 1837−1839.
(11) Thuéry, P.; Masci, B. *CrystEngComm* **2012**, *14*, 131−137.
(12) (a) Batten, S. R.; Robson, R. *Angew. Chem., Int. Ed.* **1998**, *37*, 1460−1494. (b) Batten, S. R. *CrystEngComm* **2001**, *3*, 67. (c) Batten, S. R. *Curr. Opin. Solid State Mater. Sci.* **2001**, *5*, 107−114. (d) Carlucci, L.; Ciani, G.; Proserpio, D. M. *Coord. Chem. Rev.* **2003**, *246*, 247−289. (e) Jiang, H. L.; Makal, T. A.; Zhou, H. C. *Coord. Chem. Rev.* **2013**, *257*, 2232−2249. (f) Yang, G. P.; Hou, L.; Ma, L. F.; Wang, Y. Y. *CrystEngComm* **2013**, *15*, 2561−2578. (g) Carlucci, L.; Ciani, G.; Proserpio, D. M.; Mitina, T. G.; Blatov, V. A. *Chem. Rev.* **2014**, *114*, 7557−7580.
(13) (a) Go, Y. B.; Wang, X.; Jacobson, A. J. *Inorg. Chem.* **2007**, *46*, 6594−6600. (b) Lis, S.; Glatty, Z.; Meinrath, G.; Kubicki, M. *J. Chem. Crystallogr.* **2010**, *40*, 646−649. (c) Wu, H. Y.; Wang, R. X.; Yang, W.; Chen, J.; Sun, Z. M.; Li, J.; Zhang, H. *Inorg. Chem.* **2012**, *51*, 3103−3107. (d) Chen, F.; Wang, C. Z.; Li, Z. J.; Lan, J. H.; Ji, Y. Q.; Chai, Z. F. *Inorg. Chem.* **2015**, *54*, 3829−3834. (e) Wang, Y.; Liu, Z.; Li, Y.; Bai, Z.; Liu, W.; Wang, Y.; Xu, X.; Xiao, C.; Sheng, D.; Diwu, J.; Su, J.; Chai, Z.; Albrecht-Schmitt, T. E.; Wang, S. *J. Am. Chem. Soc.* **2015**, *137*, 6144−6147.
(14) Hooft, R. W. W. *COLLECT*; Nonius BV: Delft, The Netherlands, 1998.
(15) Otwinowski, Z.; Minor, W. *Methods Enzymol.* **1997**, *276*, 307−326.
(16) Sheldrick, G. M. *Acta Crystallogr., Sect. A: Found. Crystallogr.* **2008**, *64*, 112−122.
(17) Sheldrick, G. M. *Acta Crystallogr., Sect. A: Found. Adv.* **2015**, *71*, 3−8.
(18) Sheldrick, G. M. *Acta Crystallogr., Sect. C: Struct. Chem.* **2015**, *71*, 3−8.
(19) Spek, A. L. *J. Appl. Crystallogr.* **2003**, *36*, 7−13.
(20) Farrugia, L. J. *J. Appl. Crystallogr.* **1997**, *30*, 565.
(21) Momma, K.; Izumi, F. *J. Appl. Crystallogr.* **2008**, *41*, 653−658.
(22) (a) Blatov, V. A.; Shevchenko, A. P.; Serezhkin, V. N. *J. Appl. Crystallogr.* **2000**, *33*, 1193. (b) Blatov, V. A.; O'Keeffe, M.; Proserpio, D. M. *CrystEngComm* **2010**, *12*, 44−48.
(23) See, for example: (a) Li, X.; Cao, R.; Sun, D.; Shi, Q.; Bi, W.; Hong, M. *Inorg. Chem. Commun.* **2003**, *6*, 815−818. (b) Frisch, M.; Cahill, C. L. *Dalton Trans.* **2005**, 1518−1523. (c) Li, B.; Gu, W.; Zhang, L. Z.; Qu, J.; Ma, Z. P.; Liu, X.; Liao, D. Z. *Inorg. Chem.* **2006**, *45*, 10425−10427. (d) Thuéry, P. *Polyhedron* **2007**, *26*, 101−106. (e) Frisch, M.; Cahill, C. L. *J. Solid State Chem.* **2007**, *180*, 2597−2602. (f) Knope, K. E.; Cahill, C. L. *Inorg. Chem.* **2007**, *46*, 6607−6612. (g) Ziegelgruber, K. L.; Knope, K. E.; Frisch, M.; Cahill, C. L. *J. Solid State Chem.* **2008**, *181*, 373−381. (h) Thuéry, P. *CrystEngComm* **2008**, *10*, 808−810. (i) Thuéry, P. *CrystEngComm* **2008**, *10*, 1126−1128. (j) Thuéry, P. *CrystEngComm* **2009**, *11*, 2319−2325. (k) Thuéry, P. *CrystEngComm* **2010**, *12*, 1905−1911. (l) Rowland, C. E.; Cahill, C. L. *Inorg. Chem.* **2010**, *49*, 6716−6724. (m) Thuéry, P. *Inorg. Chem.* **2011**, *50*, 1898−1904. (n) Andrews, M. B.; Cahill, C. L. *CrystEngComm* **2011**, *13*, 7068−7078. (o) Knope, K. E.; Kimura, H.; Yasaka, Y.; Nakahara, M.; Andrews, M. B.; Cahill, C. L. *Inorg. Chem.* **2012**, *51*, 3883−3890.
(24) (a) Borkowski, L. A.; Cahill, C. L. *Inorg. Chem.* **2003**, *42*, 7041−7045. (b) Borkowski, L. A.; Cahill, C. L. *Cryst. Growth Des.* **2006**, *6*, 2241−2247. (c) Borkowski, L. A.; Cahill, C. L. *Cryst. Growth Des.* **2006**, *6*, 2248−2259. (d) Thuéry, P. *Cryst. Growth Des.* **2011**, *11*, 2606−2620.
(25) Knope, K. E.; de Lill, D. T.; Rowland, C. E.; Cantos, P. M.; de Bettencourt-Dias, A.; Cahill, C. L. *Inorg. Chem.* **2012**, *51*, 201−206.
(26) Brachmann, A.; Geipel, G.; Bernhard, G.; Nitsche, H. *Radiochim. Acta* **2002**, *90*, 147−153.
(27) (a) Burrows, H. D.; Miguel, M.; da, G. *Adv. Colloid Interface Sci.* **2001**, *89*−*90*, 485−496. (b) Formosinho, S. J.; Burrows, H. D.; Miguel, M.; da, G.; Azenha, M. E. D. G.; Saraiva, I. M.; Ribeiro, A. C. D. N.; Khudyakov, I. G.; Gasanov, R. G.; Sarakha, M. *Photochem. Photobiol. Sci.* **2003**, *2*, 569−575. (c) Redmond, M. P.; Cornet, S. M.; Woodall, S. D.; Whittaker, D.; Collison, D.; Helliwell, M.; Natrajan, L. S. *Dalton Trans.* **2011**, *40*, 3914−3926. (d) Zhang, Y.; Karatchevtseva, I.; Price, J. R.; Aharonovich, I.; Kadi, F.; Lumpkin, G. R.; Li, F. *RSC Adv.* **2015**, *5*, 33249−33253.
(28) (a) Alsobrook, A. N.; Zhan, W.; Albrecht-Schmitt, T. E. *Inorg. Chem.* **2008**, *47*, 5177−5183. (b) Heine, J.; Müller-Buschbaum, K. *Chem. Soc. Rev.* **2013**, *42*, 9232−9242.

DOI: 10.1021/acs.inorgchem.5b01323
Inorg. Chem. 2015, 54, 8093−8102